ELSEVIER

Materials Science and Engineering A 452–453 (2007) 228–234

MATERIALS SCIENCE & ENGINEERING A

www.elsevier.com/locate/msea

Study for multilayer piezoelectric composite structure as displacement actuator by Moiré interferometry and infrared thermography experiments

Wei Qiu [a], Yi-Lan Kang [a,*], Qing-Hua Qin [b], Qing-Chi Sun [c], Fang-Yu Xu [a]

[a] *Department of Mechanics, Tianjin University, Tianjin 300072, China*
[b] *Department of Engineering, Australian National University, Canberra, ACT 0200, Australia*
[c] *Department of Material Engineering, Tianjin University, Tianjin 300072, China*

Received 5 January 2006; received in revised form 17 October 2006; accepted 18 October 2006

Abstract

Multilayer piezoelectric structures are widely applied as a smart structure in precise apparatus. When the structure is in service, fractures often occur near the internal electrode layers. To analyze this issue, a multilayer piezoceramic structure used as displacement actuator is investigated both experimentally and numerically in this paper. Through Moiré interferometry experiment, the plane displacement distribution of the structure is obtained, which is holistically consistent with and locally more acute than the one obtained from finite element simulation. This displacement field shows there is considerable non-uniform deformation in the structure, which is caused by electric field concentration near the edge of the internal electrode, and consequently induces serious stress concentration there that may finally lead to significant damage or failure of the structure in its working environment. Furthermore, the thermal phenomena in piezoelectric structures were measured experimentally by applying infrared thermography. The thermo-concentration around interface crack and inside internal microdefects may intensify non-uniform stress distribution and make structure more vulnerable in its working environment. Hence it should be taken into account in the investigation of piezoelectric structures henceforth.

Keywords: Moiré interferometry; Infrared thermography; Multilayer piezoelectric structure

1. Introduction

Multilayer piezoelectric ceramic displacement actuator is a typical smart composite structure and has wide application in precise apparatus [1,2]. For such structures, fracture often occurs near the internal electrode layers, and cracks are always initiated at the electrode edges when it is in service [3,4]. These may lead to functional invalidation, which significantly reduce the stability, reliability, and applied universality of this structure [2,5]. Therefore, it is important to study mechanisms of fracture and stress concentration, and to enhance strength and reliability designing for such structures.

During the past decades, numerous works have been reported in the literature on fracture and reliability of piezoelectric structures [3,6–11]. However, most of these works were based on theoretical modelling and numerical simulation. It seems that there is a lack of elaborate experimental investigation in this direction. In particular, there is no existing experimental work regarding thermal effects on mechanical performance of multilayer piezoelectric composite structures. For fracture and failure analysis, Qin et al. [12] presented a micromechanics model for evaluating effective properties of *thermopiezoelectric materials with microcracks*. Fu et al. [13] found from the experiment on the fracture of piezoelectric material that energy dissipation under electrical loading is greater than that under mechanical loading. Du's experiments [14] verified that temperature of the piezoceramics is related to the frequencies of electric loading. Gu and Yu [15] analyzed the thermal effect of piezoelectric medium for anti-plane problem theoretically. From the discussion above, it is obvious that very little experimental work has been reported on study locally precise deformation and thermal effect of piezoelectric structure through locally full-field microscopical methods.

* Corresponding author. Tel.: +86 22 87401572; fax: +86 22 87894001.
E-mail addresses: YLKang@public.tpt.tj.cn, Daniell_q@hotmail.com (Y.-L. Kang).

0921-5093/$ – see front matter © 2006 Elsevier B.V. All rights reserved.
doi:10.1016/j.msea.2006.10.165

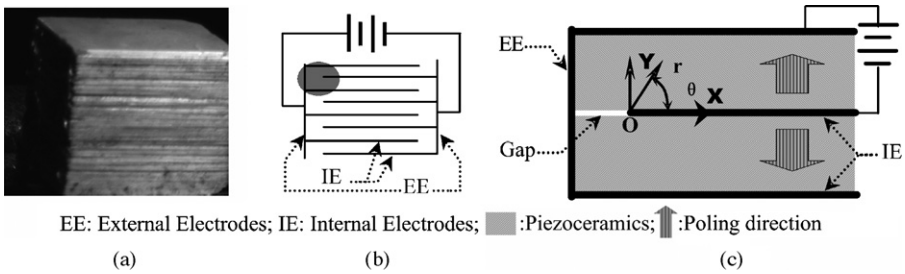

Fig. 1. Illustration of the multilayer piezoelectric structure. (a) Photograph of practical element; (b) planer simplified structure; (c) enlarged illustration near the edge of internal electrode (viz. point O).

This paper investigates a multilayer piezoceramics structure, which is used as displacement actuator, by means of Moiré interferometry, infrared thermography and finite element simulation. Firstly, plane displacement distribution of the structure was captured by using Moiré interferometry approach. Then, the thermal effect of fracture behavior of the piezoceramics structure is analyzed by applying infrared thermography. Finally, the structural strength is discussed based on the experimental and numerical results.

2. Multilayer piezoelectric structure and specimen

2.1. Structure and mechanism

The multilayer piezoelectric composite structure is illustrated in Fig. 1a and it can be simplified as plane model [4] shown in Fig. 1b. The structure is composed of shunt-wound piezoceramics layers and thin argent electrodes distinguished into external and internal ones. When loading voltage on external electrodes, each layer will be applied an electric field by internal electrodes and induced to deform following principle of electrostriction [9]:

$$\begin{cases} (\varepsilon_z =)\varepsilon_x = d_{31}E_y \\ \varepsilon_y = d_{33}E_y \end{cases} \quad (1)$$

where E_y is the electric field intensity in y-direction; ε_x, and ε_y the electrostrictive strains in the x- and y-directions, espectively; d_{31} and d_{33} are the piezoelectric strain constants. Hence, the holistic displacement is the accumulation of all layers' deformation.

On the interface between any two layers there is a gap from the edge of the internal electrode to the inner surface of the external electrode. Due to the existence of such gap, the two polar electrodes and even the whole structure can be free of short circuits. When the structure is in service (i.e. in the working environment), however, fracture usually occurs near the tip of the gap, or rather, edge of the internal electrode which is enlarged as shown in Fig. 1c.

2.2. Specimen material and loads

The geometrical dimensions of the multilayer structure specimen are listed in Table 1. The piezoelectric material of the specimen is plumbic-zirconate–titanate ceramic [$Pb(Zr_{x\,(0.50\le x\le 0.54)}\ Ti_{1-x})O_3$] or PZT for short, which belongs to transversely isotropic materials. The material constants of PZT are listed in Table 2.

Table 1
Geometrical dimensions of specimen

Electrode length (mm)	17.88
Width (mm)	7.40
Height (mm)	2.31
Thickness per layer (mm)	0.77

Table 2
Material constants

Elastic compliance ($\times 10^{-12}$ m^2/N)	
s^E_{11}	16.4
s^E_{12}	−5.78
s^E_{13}	−7.5
s^E_{33}	18.8
s^E_{44}	50
Piezoelectric strain constants ($\times 10^{-12}$ C/N)	
d_{31}	−190
d_{33}	430
d_{15}	730
Dielectric constants ($K^\sigma_0 = 8.85 \times 10^{-12}$ F/m)	
K^σ_{11}/K^σ_0	1720
K^σ_{33}/K^σ_0	1700

In the experiments described below, the specimens were loaded by uniform external loads. Furthermore, according to the actual working environment of the multilayer piezoelectric displacement actuator, the specimens were assumed to be loaded by the external electric field only. In other words, no external mechanical loading was applied to the structure. In this study, two typical loads are considered: firstly the so-called positive loading, for which an electric field is applied on each layer in the poling direction, and secondly negative loading. The magnitude of the electric loading is 1000 kV/m in the positive loading condition and −1000 kV/m in the negative loading condition.

3. Experiments and numerical simulation

3.1. Moiré interferometry experiment

Moiré interferometry experiment has been carried out to detect the plane deformation of the multilayer structure precisely. Moiré interferometry is a highly sensitive optical method using coherent laser light and its principle [16] is depicted briefly

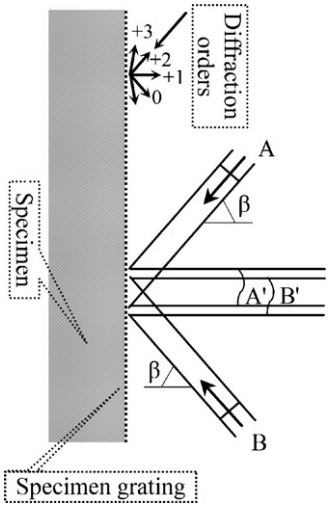

Fig. 2. Principle of Moiré interferometry.

in Fig. 2. In this method, two coherent laser light beams A and B illuminate the specimen grating and diffract into A′ and B′, respectively. When the specimen is loaded to deform, A′ and B′ will interfere and form a Moiré fringe pattern. The Moiré fringe pattern is a contour map of displacement and represents the plane displacement field of the specimen in a particular direction, such as displacement V in y-direction (or displacement U in x-direction). The value of V at a point (x, y) can be obtained from the fringe using the relationship $V(x, y) = N_y/4f_y$, where N_y is the order of Moiré fringes in fringe pattern at the point and f_y the specimen frequency in y-direction. Thus the displacement sensitivity (the plane displacement that a fringe indicated), is $1/4f_y$. Moreover, by applying phase-shift and multiplication technique [17], it could be promoted to $1/(4Mf_y)$, where M is a multiple factor of multiplication operation.

The optical system of phase-shift Moiré interferometry used in this work is shown in Fig. 3. Before loaded with high voltage, specimens were required to be airproofed and insulated by silicon rubber to avoid electric shock. Fig. 4 shows the fringe pattern near the edge of the electrode in the multilayer structure specimen under +1000 kV/m electric field loading, where

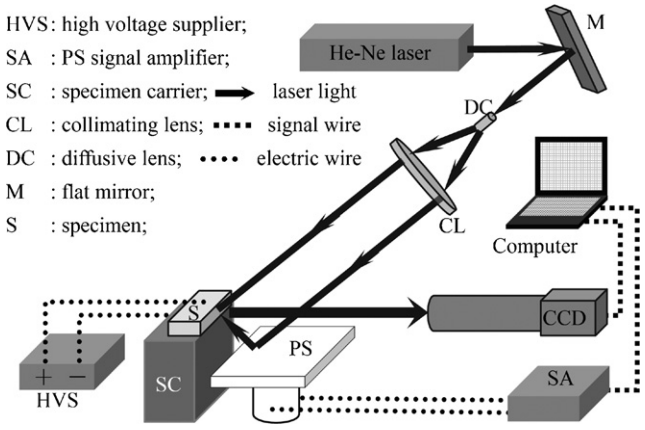

Fig. 3. Phase-shift Moiré interferometry optical system.

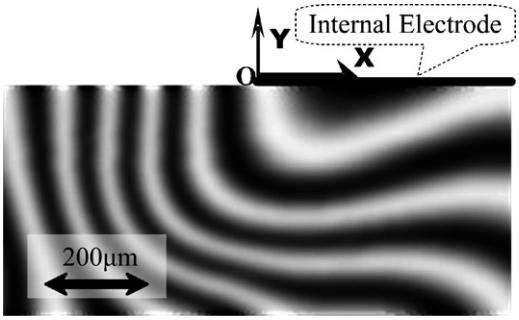

Fig. 4. Fringe pattern near the edge of the internal electrode (+1000 kV/m, $M = 4$).

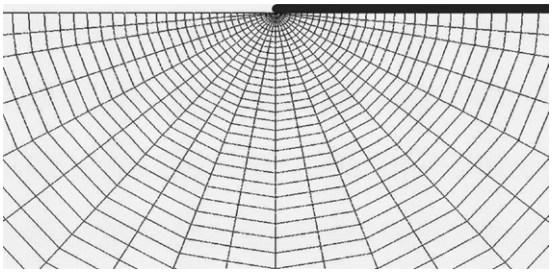

Fig. 5. Finite element mesh near the edge of the internal electrode.

$4f_y = 2400$ lines/mm and $M = 4$, therefore the displacement sensitivity is 0.108 μm/fringe.

3.2. Numerical simulation

To verify the accuracy of the results obtained from the experiments and applicability of finite element method to this problem, numerical simulations were performed by means of finite element package ABAQUS (V6.2). In finite element simulation, the configuration of the multilayer structure is divided into 6460 four-node plane elements. In order to calculate the stress and electric field distributions at the edge of the electrode accurately, the mesh density was increased near the edge of the electrode (see Fig. 5). The minimal size of the elements near the edge of the internal electrode was 2 μm × 6 μm. Fig. 6 shows the displacement contour map in the poling direction loaded with +1000 kV/m, whose local region and loading condition are the same as those in Fig. 4.

By comparing Fig. 4 with Fig. 6 it can be seen that, as a whole, the plane displacement field recorded by Moiré interfer-

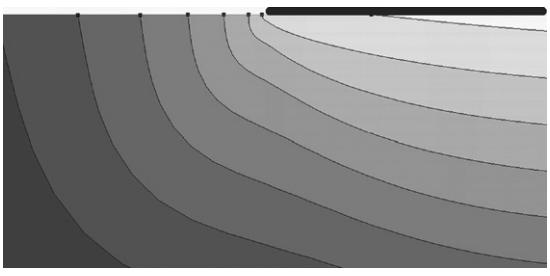

Fig. 6. Displacement contour near the edge of the internal electrode (+1000 kV/m).

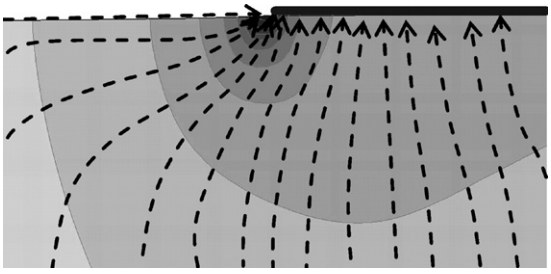

Fig. 7. Distribution of electric field and fluxline near the edge of the internal electrode.

ometry experiment is consistent with that obtained by numerical simulation both in tendency and magnitude of variation. It is evident that numerical simulation could approximately predict the veritable events such as displacement field (Fig. 6), the electric field (Fig. 7) and principal stress distribution (Fig. 8) in multilayer piezoelectric structures. However, the experimental data are more acute than the numerical ones near the edge of the internal electrode, which will be analyzed later in this paper. Besides, the trends of the results in negative loading condition are similar to those in positive loading condition, thus it is unnecessary to discuss their difference.

3.3. Discussion on the strength and damage mechanism

Structural damages are frequent in the engineering application of piezoelectric displacement actuators. Therefore, it is necessary to analyze the strength and discuss the damage mechanism based on the experimental and numerical results obtained.

For the structure used as displacement actuator, it is loaded by the electric field due to the electric potential difference between the electrodes. The electric field is homogeneous inside each layer except near the edge of the internal electrode (namely point O), where the electric field distribution is can be calculated by [4]:

$$\begin{Bmatrix} E_x \\ E_y \end{Bmatrix} = \frac{K_E}{\sqrt{2\pi r}} \begin{Bmatrix} \cos\left(\frac{\theta}{2}\right) \\ \sin\left(\frac{\theta}{2}\right) \end{Bmatrix} \tag{2}$$

where E_x and E_y are, respectively, the magnitude of the electric field in the x- and y-direction; K_E is the electric intensity factor; $\sin(\theta/2)$, $\cos(\theta/2)$ are the so-called angle distributing functions of the electric field.

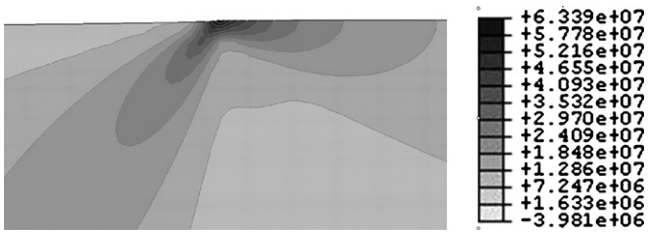

Fig. 8. Distribution of principal stress near the edge of the internal electrode (+1000 kV/m).

Using Eq. (2), the intensity and flux-line of electric field around the edge of the electrode (viz. point O) can be determined and the results are listed in Fig. 7. It can be seen from Fig. 7 that, the orientation of electric field is, mathematically, expressed in terms of polar angle θ, and the singularity of the electric field is in the order of minus square root of r. Here r is the distance from crack tip to the point under consideration. While physically, the flux-line flows densely and the magnitude increases rapidly when approaching point O, both of the density and the magnitude of the flux-line flow indicate that electric field concentration becomes increasingly drastic near the electrode edge.

It is obvious from Eq. (1) that the electric field applied to the piezoelectric layers can induce electrostrictive strains that are determined by the piezoelectric constants and the intensity of electric field only. Consequently, the electric field concentration around the point O will produce non-uniform electrostriction, and in turn cause non-uniform elastic deformation. This is substantiated by both the experimental result (Fig. 4) and the numerical solution (Fig. 6). In particular, the displacement contours are approximately parallel to the electrodes when the position is far from the point O, while it is in bending about 90° when near the edge of the internal electrode.

Such deformation, however, is constrained by the surrounding materials, and consequently leads to non-uniform and incompatible stress, even stress concentration. Fig. 8 gives the principal stress distribution in the region near the electrode edge (+1000 kV/m). It can be seen that the stress distribution is complicated and the maximum can reach 63 MPa at the electrode edge. Moreover, the high stress concentration exists in a very small region only and decreases rapidly along with an increase in the distance from the electrode edge. From this point of view and in view of numerous microdefects existing in multilayer piezoelectric structures as noted by Winzer and Shankar [2], the stress concentration near the electrode edge may induce microdefects likely to extend and finally lead to significant damage or failure of the structure.

In fact, the real stress concentration near the edge of the internal electrode should be more serious than that shown in Fig. 8 as the deformation obtained from Moiré interferometry experiment is more acute than that obtained from finite element simulation in the vicinity of the electrode edge. This difference is indicated as the effects of thermal phenomena near the electrode edge by the further infrared microthermography experiments as follows.

4. Infrared thermography experiments

The discussion above concerned experiments and numerical simulation on electric and elastic fields only. For multilayer piezoelectric structures, however, thermal effect on structural performance is also of importance. As there is no report about experimental investigation on thermal effect in multilayer piezoelectric structures in the literature, a series of infrared microthermography experiments are preformed to investigate how the temperature change can affect the structural performance and the mechanism causing distinction between experimental and numerical simulating data when the thermal effect is ignored.

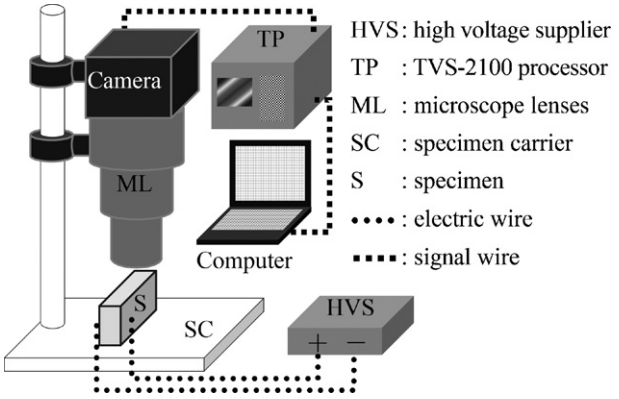

Fig. 9. Microthermography system.

Table 3
Main parameters of the thermograph system

Thermometric sensitivity (°C)	0.05
Scanning frame (f/s)	30
Spatial resolution (μm)	25
Metrical infrared wavelength (μm)	3

4.1. Experimental principle and procedure

Thermography is a technique to test the surface temperature of a certain object by applying thermographic system. The main principle of thermography is described as below [18,19]. The radiation pattern of infrared energy emitted by any object corresponds to its surface temperature distribution. This pattern is invisible to the naked eye, but it can be detected by infrared camera. The main processor (such as TVS-(2000) ST processor) receives thermal data from the camera and then converts them into visual digital image known as thermal image. Hereby, infrared camera, main processor and other accessories such as monitor, printer and even computer make up a general thermographic system (Fig. 9). Furthermore, microthermographic system is the apparatus especially for the measurement of the micro-object, like the specimen in this paper, which cannot be tested unless equipped with microscope lenses in front of the infrared camera. The microthermographic system used in the experiment is illustrated in Fig. 9, whose main parameters are listed in Table 3.

In addition to the multilayer structure specimen, another specimen with an internal crack (see Fig. 10) is analyzed in the thermographic experiment. The internal crack does not adjoin or close to any boundary of the specimen, which eliminates the influence and disturbance from electrodes. Both two specimens have the same geometrical dimensions and material components (listed in Tables 1 and 2, respectively). Moreover, the specimens are subjected to the alternating electric loading (alternating between the positive and negative loading condition) in the frequency that verge on its resonance frequency (about 200 Hz) to intensify the thermal phenomena.

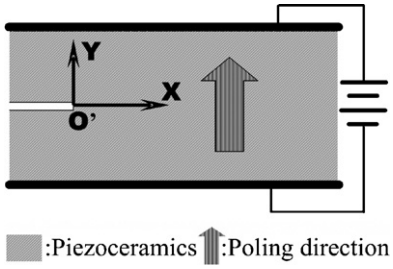

Fig. 10. Illustration of the internal crack specimen.

Besides, restricted by the spatial resolution, temporal and thermometric sensitivity and other factors of the thermographic system [20], any temperature value is an average of the ambient region (25 μm × 25 μm in TVS-(2000) system) around the respective point. Therefore, the tests in this paper above can semi-quantitatively describe the real thermal distributions in the specimens.

4.2. Results and discussion

Fig. 11 gives the thermal images of the specimens, while Figs. 12 and 13 show the temperature distributions along the *x*- and *y*-axes in multilayer structure specimen and the one with internal crack, respectively. It can be seen from Figs. 11a and 12 that a thermo-concentration exists around the electrode edge (say point O) and the temperature rises sharply when the location approaches the point O. Meanwhile, from Figs. 11b and 13, another thermo-concentration near the crack notwithstanding without electrode was observed. Besides, the points inside the crack (outside the specimen) have higher temperatures than those inside the specimen.

These thermal phenomena are neither isolated nor inoperative to the structure in service. In fact, the causes of thermal phenomena and even thermo-concentration above could be

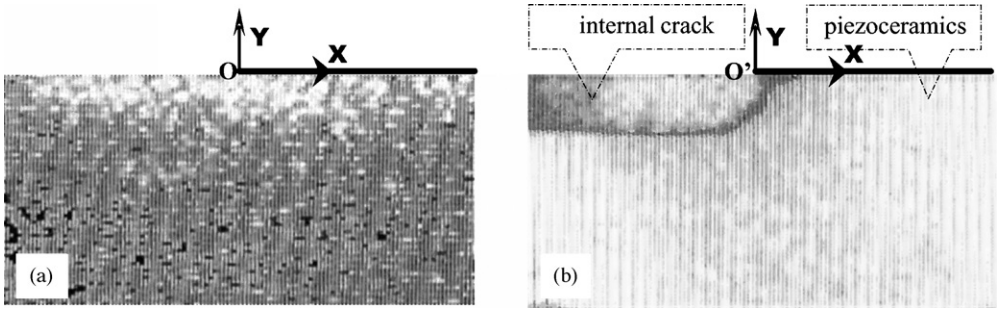

Fig. 11. Infrared thermal images in alternating loading condition. (a) Around O in multilayer structure specimen; (b) around O′ in internal crack specimen.

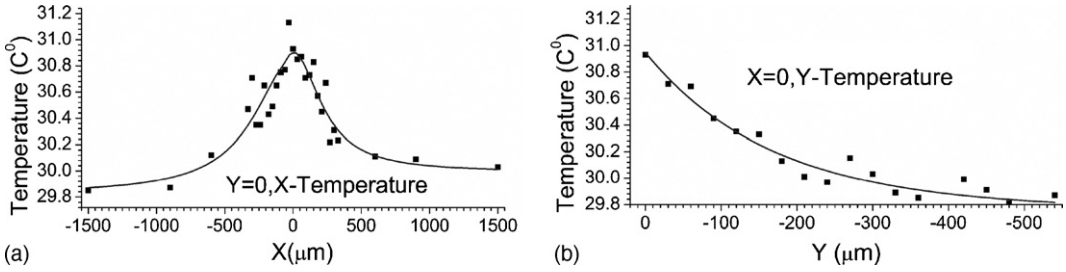

Fig. 12. Temperature distributions along the *x*- and *y*-directions of multilayer structure specimen in alternating loading condition.

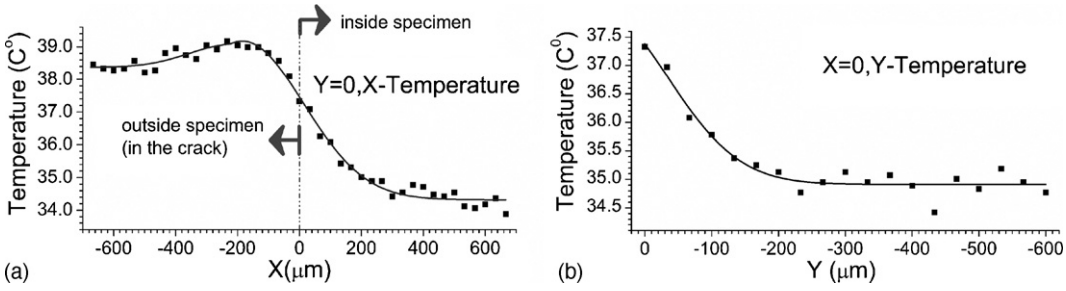

Fig. 13. Temperature distributions along the *x*- and *y*-directions of prefabricated internal crack specimen in alternating loading condition.

likely attributed to the coupling of multifactor including the electrical field and stress concentration discussed above, vibration and nonlinear behavior of the materials [15]. In return, thermal phenomena may affect the structure multiformly in addition to inflecting the nonlinear characteristics of material. The thermo-concentration at the electrode edge may intensify the non-uniform deformation and then the stress concentration there. At the same time, numerous microdefects locate inside the structure everywhere, and each of them can be regarded as a mini sample of internal crack shown in Fig. 10. Among them, the ones close to the electrode edge bear more serious electrical field and stress, due to the electrical and stress concentrations, than those far from the edge. Hence, they may behave more acute local thermo-concentration, and then more non-uniform deformation and stress. All above make the structure more vulnerable in its working environment and should be taken into account in the investigation of piezoelectric composite structures henceforth.

5. Conclusions

This paper investigates a typical multilayer piezoelectric composite structure by means of Moiré interferometry experiments, thermography experiments and numerical simulations. The major aspects of the work are as follows.

(3) The plane displacement field obtained by Moiré interferometry experiment shows that there is considerable non-uniform deformation in the multilayer piezoelectric composite structure. This non-uniform deformation is caused by electric field concentration near the edge of the internal electrode and it can induce serious stress concentration there, which may finally lead to significant damage or failure of this structure in its working environment.

(3) The holistic similarity between the experimental and simulated results confirms that numerical simulation can predict the veritable events in piezoelectric composite structures on the condition of proper simplification.

(3) The thermal phenomena in piezoelectric composite structures are measured experimentally. The thermo-concentration around internal crack and interface crack (viz. the internal electrode edge in this paper) may intensify the non-uniform deformation and the stress concentration in the structure, and it should be taken into account in the investigation of piezoelectric composite structures henceforth.

Acknowledgements

The authors would like to acknowledge the financial support of the National Natural Science Foundation of China (SN: 10232030 and SN: 10572102) and the 2005 Endeavour Australia Cheung Kong Award.

References

[1] K. Uchino, Am. Ceram. Soc. Bull. 65 (1986) 647–652.
[2] S.R. Winzer, N. Shankar, J. Am. Ceram. Soc. 72 (1989) 2246–2257.
[3] Z. Suo, C.M. Kuo, D.M. Barnett, J.R. Willis, J. Mech. Phys. Solids 40 (1992) 739–765.
[4] W. Yang, Z. Suo, J. Mech. Phys. Solids 42 (1994) 649–663.
[5] X. Gong, Z. Suo, J. Mech. Phys. Solids 44 (1996) 751–769.
[6] H.G. Beom, S.N. Atluri, Int. J. Fract. 75 (1996) 163–183.
[7] C.L. Hom, N. Shankar, Int. J. Solids Structs. 33 (1996) 1757–1779.
[8] Q.H. Qin, S.W. Yu, Int. J. Solids Struct. 34 (1997) 581–590.
[9] Q.H. Qin, Fracture Mechanics of Piezoelectric Materials, WIT Press, Southampton, 2001.
[10] B.H. Sun, Y. Qiu, Smart Mate. Struct. 13 (2004) 337–349.
[11] W. Qiu, Y.L. Kang, Q.C. Sun, Q.H. Qin, Y. Lin, Acta Mech. Solid. Sin. 17 (2004) 323–329.
[12] Q.H. Qin, Y.W. Mai, S.W. Yu, Inter. J. Fract. 91 (1998) 359–371.
[13] R. Fu, C.F. Qian, Y.Z. Tong, Appl. Phys. Lett. 76 (2000) 126–128.

[14] T.B. Du, Thesis of PhD UIUC in USA, 2001.
[15] B. Gu, S.W. Yu, Comput. Mater. Sci. 18 (2003) 628–632.
[16] D. Post, B. Han, P. Ifju, High Sensitivity Moiré Experimental Analysis for Mechanics and Materials, Springer-Verlag, Berlin, 1994.
[17] Y.L. Kang, D.H. Fu, G.F. Wang, S.W. Yu, X.J. Pan, J. Strain Anal. Eng. Anal. 37 (2002) 281–287.
[18] M. Clark, D.M. McCann, M.C. Forde, NDT&E Inter. 35 (2002) 83–94.
[19] R.F. El-Hajjar, R.M. Haj-Ali, Exp. Techn. 28 (2004) 19–22.
[20] M. Grecki, J. Pacholik, B. Wiecek, A. Napieralski, Microelectron. J. 28 (1997) 337–347.